LAWRENCE
LIVERMORE
NATIONAL
LABORATORY

UCRL-PROC-215970

Spin distribution in neutron induced preequilibrium reactions

D. Dashdorj, T. Kawano, M. Chadwick, M. Devlin, N. Fotiades, R. O. Nelson, G. E. Mitchell, P. E. Garrett, U. Agvaanluvsan, J. A. Becker, L. A. Bernstein, R. Macri, W. Younes

October 6, 2005

International School of Contemporary Physics
Ulaanbaatar, Mongolia
August 3, 2005 through August 15, 2005

Spin distribution in neutron induced preequilibrium reactions

D. Dashdorj*
North Carolina State University, Raleigh, NC 27695 and
Lawrence Livermore National Laboratory, Livermore, CA 94551

T. Kawano, M. Chadwick, M. Devlin, N. Fotiades, and R. O. Nelson
Los Alamos National Laboratory, Los Alamos, NM 87545

G. E. Mitchell
North Carolina State University, Raleigh, NC 27695 and
Triangle Universities Nuclear Laboratory, Durham, NC 27708

P. E. Garrett,† U. Agvaanluvsan, J. A. Becker, L. A. Bernstein, R. Macri, and W. Younes
Lawrence Livermore National Laboratory, Livermore, CA 94551

The preequilibrium reaction mechanism makes an important contribution to neutron-induced reactions above $E_n \sim 10$ MeV. The preequilibrium process has been studied exclusively via the characteristic high energy neutrons produced at bombarding energies greater than 10 MeV. We are expanding the study of the preequilibrium reaction mechanism through γ-ray spectroscopy. Cross-section measurements were made of prompt γ-ray production as a function of incident neutron energy (E_n = 1 to 250 MeV) on a ^{48}Ti sample. Energetic neutrons were delivered by the Los Alamos National Laboratory spallation neutron source located at the Los Alamos Neutron Science Center facility. The prompt-reaction γ rays were detected with the large-scale Compton-suppressed Germanium Array for Neutron Induced Excitations (GEANIE). Neutron energies were determined by the time-of-flight technique. The γ-ray excitation functions were converted to partial γ-ray cross sections taking into account the dead-time correction, target thickness, detector efficiency and neutron flux (monitored with an in-line fission chamber). Residual state population was predicted using the GNASH reaction code, enhanced for preequilibrium. The preequilibrium reaction spin distribution was calculated using the quantum mechanical theory of Feshbach, Kerman, and Koonin (FKK). The multistep direct part of the FKK theory was calculated for a one-step process. The FKK preequilibrium spin distribution was incorporated into the GNASH calculations and the γ-ray production cross sections were calculated and compared with experimental data. The difference in the partial γ-ray cross sections using spin distributions with and without preequilibrium effects is significant.

PACS numbers: 21.10.-i, 24.60.Dr, 25.40.-h, 25.40.Fq, 27.40.+z

I. INTRODUCTION

Cross sections of many reactions, including preequilibrium reactions, have important practical applications, from the design of fission and fusion reactors to space and astrophysical research. It is often necessary to measure, or if measurement is not possible, to estimate nuclear cross sections both at low and high energies to moderate accuracy. The spin transfer in preequilibrium neutron-induced reactions may play an important role in the reaction cross sections. The spin distribution in the residual nucleus can be deduced from a comparison of the relative population of low-lying states with different spins (measured using the GEANIE array), with the predictions from state-of-the-art Hauser-Feshbach codes incorporating preequilibrium models. Preequilibrium reactions are important when incident neutron energies are above $\approx$ 10 MeV, as evidenced by e.g., fast neutron emission. The spin distribution is predicted by the theoretical calculations. However, there are no experimental data to compare with the theoretical calculations of the spin distribution in the residual nucleus in the region of the preequilibrium reactions. The powerful γ-ray array GEANIE coupled with the intense neutron beam at WNR/LANSCE brings a new tool for the investigation of the preequilibrium process. The partial γ-ray cross sections for low-lying states with different J^π were measured as a function of neutron energy. These cross sections were interpreted with the aid of reaction modeling to determine the transferred spin distribution. Increased understanding of the preequilibrium mechanism should improve reaction model predictions.

Preequilibrium reactions take place on a time scale that is between the direct and compound processes. Since preequilibrium emission occurs before the composite nucleus reaches its equilibrated state, on average the preequilibrium particles are emitted with more energy than the particles following the formation of a compound nu-

*Electronic address: dashdorj1@llnl.gov
†Present address: Department of Physics, University of Guelph, ON N1G 2W1, Canada

cleus. Although the preequilibrium mechanism has been studied in the past, it is not completely understood. Measuring the prompt reaction γ rays as a function of incident neutron energy provides improved understanding of the spins populated by the preequilibrium reaction; this information is obtained by studying angular momentum information for the γ-ray cascades in the residual nucleus. Several models have been developed that describe the preequilibrium process: the cascade model [1], the exciton model [2], the FKK model [3], the HMS [4] model, the TUL [5] model and NWY [6] model. The quantum-mechanical theory of Feshbach, Kerman, and Koonin (FKK) describes inelastic multistep processes in nucleon-induced reactions. This model allows a direct calculation of the spin distributions of residual nuclei remaining after preequilibrium emission. The magnitude of preequilibrium emission at various incident neutron energies affects the angular momentum distribution of the populated states in the excited residual nucleus. This distribution is different from that arising from equilibrium neutron emission alone. To study the spin distribution of the residual nucleus in preequilibrium reactions, one needs to tag states with specific angular momentum. An example would be to compare the population of 6^+ states to 2^+ states in the ground state band as a function of incident neutron energy in a region where preequilibrium is expected to dominate.

The experimental details of the measurement of prompt γ rays from neutron-induced reactions and a description of the experimental devices are presented in Section II. In Section III the analysis of the experimental data is described. The next section includes a description of the Hauser-Feshbach Statistical Model calculations. Partial γ-ray cross sections are presented and compared with Hauser-Feshbach statistical model calculations. Also the spin distribution of states populated by the preequilibrium reactions and the comparison of experimental and theoretical predictions are discussed. Section V summarizes the results of this work, and provides suggestions for future research.

II. EXPERIMENTAL SETUP

The experimental data were obtained at the Los Alamos Neutron Science Center (LANSCE) Weapons Neutron Research (WNR) facility. At the WNR facility, spallation neutrons are produced by bombarding a natural W target with an 800-MeV pulsed proton beam from the LANSCE linac. The pulsed proton beam consists of micropulses 1.8-μs apart, bunched into macropulses 625 μs in duration. Spallation neutrons with energies ranging from a few keV to nearly 800 MeV are produced. The "white" neutron spectrum decreases nearly exponentially with increasing neutron energy. Beam-hardening material (1.5 cm of lead) was placed in the neutron flight path. The neutrons were collimated to a circular beam spot about 1.5 cm in diameter at the scattering-sample position. The scattering sample consisted of 3.3 grams of TiO_2 in the form of disks 2.4 cm diameter, enriched to 99.81% in ^{48}Ti. The γ rays were detected with the GEANIE (GErmanium Array for Neutron Induced Excitations) spectrometer, located about 20 m from the neutron source on the 60° right flight path. For this experiment, the GEANIE spectrometer consisted of 11 planar and 15 25% High-purity Ge (HPGe) coaxial detectors. All of the planars and 9 of the coaxial detectors were equipped with Compton suppression shields. The detectors were situated at a distance of $\approx$ 14 cm from the focal point where the scattering sample is located. The planar detectors were used to measure γ rays with energies less than 1 MeV and the coaxial detectors measured γ rays with energies up to 4 MeV. The planar detectors were arranged in rings at angles of 27.4° (four detectors), 58.4° (two detectors), 128.0° (one detector), and 142.7° (four detectors) with respect to the neutron beam direction. The coaxial detectors were arranged in rings at angles of 56.6° (two detectors), 77.7° (two detectors), 100.5° (four detectors), and 129.5° (one detector). The six remaining coaxial detectors were unsuppressed and their events were analyzed only in $\gamma\gamma$ coincidence mode. The data from the suppressed detectors were collected in singles-and-higher-fold mode, resulting in a total array rate of $2-3$ kHz. For each unsuppressed γ-ray event, a master gate window of 20 μs was opened during which all unsuppressed pulses from the Ge detectors were processed. The data stream consisted of a bit determining whether the event occurred in or out of the macropulse, the time relative to the start of the macropulse (recorded in 100 ns intervals), energy E_γ, and (if in beam) time t_γ relative to the proton micropulse for each detector which recorded an event. The efficiency of the array has been calibrated through a series of source measurements, supplemented by detailed modeling [7] using the transport code MCNP [8].

A fission chamber consisting of ^{235,238}U foils [9] was located 2 m upstream from the GEANIE spectrometer. The neutron flux was determined using these fission chambers. Neutron energies were determined by the time-of-flight (TOF) technique, using the detection time of the "flash" of γ rays caused by the spallation reaction with respect to the beam rf signal as a reference marker. The detection time of γ rays produced by neutrons interacting with the sample was used to calculate the TOF of the neutrons relative to the γ-flash detection time. Similarly, signals from the fission chamber were used to provide a flight time relative to the γ-flash detection time (also observed in the fission chamber).

III. DATA ANALYSIS

The data were collected for about 6 days and a total of about 4.6×10^8 single- and higher-fold events were recorded. There were also separate experimental runs with a target "sandwiched" between a pair of 5-mil nat-

ural iron foils to validate the experimental technique and system consistency. During data playback, events were separated into beam-on and beam-off matrices. Two-dimensional matrices of E_γ vs. TOF and $\gamma\gamma$ coincidences were generated. In order to improve statistics, data from detectors of a particular type (planar or coaxial) were summed. The energy calibration was performed using the energies of well-known lines in ^{48}Ti and other isotopes in the beam-on data for each set of detectors. Neutron energies were determined using the TOF technique.

The excitation functions were obtained by applying TOF gates 15 ns wide on the γ-ray events in the interval to E_n = 1 to 250 MeV. For each TOF bin, a 1D γ-ray pulse-height spectrum was generated and fitted with the computer code XGAM [10] with peak shape parameters and background levels determined from a global fit to the spectrum. Fitted peaks in the spectrum were identified by comparison with accepted γ-ray energies, tabulated in the NUDAT database [11]. Partial γ-ray cross sections for transitions were obtained using the following formula

$$\sigma_\gamma(E_n) = (1+\alpha_\gamma) * \frac{\epsilon_{fc}}{\epsilon_{Ge}} * \frac{LT_{fc}}{LT_{Ge}} * \frac{1}{a_s}\frac{A_\gamma}{N_n}, \qquad (1)$$

where α_γ is the internal conversion coefficient, ϵ_{Ge} and ϵ_{fc} are the detection efficiency of the Germanium detectors and fission chamber, LT_{Ge} and LT_{fc} are the live times of the Germanium detectors and the fission chamber, a_s is the areal density of the ^{48}Ti sample, A_γ the γ-ray peak area, and N_n the number of neutrons counted in the fission chamber.

The internal conversion coefficients are taken from the NUDAT [11] database. The neutron flux used in Eq. (1) can be determined from either the ^{235}U or the ^{238}U foil in the fission chamber. Throughout this paper, the ^{238}U foil has been used consistently to extract partial γ-ray cross sections, in order to avoid the wrap-around problem arising in the incident neutron beam structure (since the flight path is long enough that low energy neutrons arrive at the target location at the same time as high-energy neutrons from a successive pulse).

The γ-ray absolute efficiency curves for planar and coaxial detectors were calculated for GEANIE data using Monte-Carlo simulations of the array [7, 8]. The calculated efficiency curves are corrected for beam-profile and target-geometry effects. The Monte-Carlo simulations for coaxial detectors were performed for γ-ray energies between 300 keV and 1800 keV. The efficiency curve for coaxial detectors was extrapolated to high energies and verified with γ-ray reference sources.

The deadtime fractions (1 − livetime) in Eq. (1) were calculated from the ratio of measured ADC and scaler counts. Total deadtimes of 62.0% and 58.0% were determined for the planar and coaxial sums, respectively, and deadtimes of 52.0% and 50.9% were obtained for the ^{235}U and ^{238}U fission foils. The systematic extraction of angular distributions for γ rays in GEANIE data is an exceedingly difficult task. The 20 detectors in the array occupy only 5 distinct angles, and the relatively short distance between sample and detector face degrades the angular resolution at those few angles.

As a validation of the experiment and the analysis technique, the partial cross section of the $2_1^+ \rightarrow 0_1^+$ transition in ^{56}Fe has been extracted from a series of runs with the ^{48}Ti sample sandwiched between 5-mil ^{nat}Fe foils. These data are compared to the cross section of 705 ± 56 mb at E_n = 14.5 MeV, evaluated by Nelson *et al.* [12].

Multiplicity two-and-higher coincidences from both the planar and coaxial detectors were sorted into a $4k\times4k$ $\gamma\gamma$ matrix. Prompt coincidence events were considerably fewer compared to single-fold data, and to maximize statistics the data from both planar and coaxial detectors were combined after converting them to the same energy range. A TOF gate corresponding to neutron energies between 1 to 12 MeV was imposed to minimize background from other reactions. To build the coincidence matrix, $\gamma\gamma$ resolving-time windows of 30 ns, 35 ns, and 40 ns were set for planar-planar, planar-coaxial, and coaxial-coaxial detector coincidences, respectively. Coincidences between γ rays provide an additional tag to eliminate extraneous information in the spectra. The coincidence matrix was analyzed to confirm γ-ray assignments and to build a partial level scheme for ^{48}Ti. A generalized background subtraction was applied to the $\gamma\gamma$ matrix that was processed using the code ESCL8R [13].

IV. THEORETICAL CALCULATIONS

Cross sections for ^{48}Ti + n reactions were calculated using the statistical Hauser-Feshbach reaction code GNASH. The general calculation method assumes that the reaction proceeds in a series of sequential two-body breakup processes. At each stage in the reaction, γ-ray and particle emission can occur and are computed using the Hauser-Feshbach theory which conserves angular momentum and parity. Width fluctuation and preequilibrium corrections including surface effects can be applied to the decay channels of the initial compound nucleus. The models utilized are expected to be most applicable for energy range 1 keV to 150 MeV. Calculations are performed for ^{48}Ti + n reactions for neutron energies between 1 MeV to 120 MeV. Spherical optical model transmission coefficients for GNASH calculations are determined with the CoH code by T. Kawano. The CoH code solves the Schrödinger equation for a given optical potential, and calculates the differential elastic scattering, reaction and total cross sections, transmission coefficients, for neutron, proton, deuteron, triton, and alpha-particle projectiles. Optical model parameters are taken from global phenomenological models. For neutrons and protons the Koning and Delaroche [14] parameters were used. The potential of Becchetti and Greenlees [15] was used for tritons and deuterons and that of Avrigeanu *et al.* [16] for α-particles. The level density theory of Ignatyuk [17] was utilized to model the statistical properties of excited nuclei. This theory is particularly ap-

propriate for analysis at higher energies since it includes damping shell effects in the level density parameter for increasing excitation energies. γ-ray transmission coefficients are calculated using one of several possible forms for γ-ray strength functions. For γ-ray emission, the strength functions and photon transmission coefficients are obtained from the giant-resonance model of Kopecky and Uhl [18]. The standard giant dipole resonance parameters are calculated for ^{48}Ti; σ_0 = 89.6 mb, E = 19.32 MeV and Γ = 5.80 MeV. For $M1$ radiation, resonance parameters are determined by $E = 41A^{-1/3}$ and Γ = 4 MeV. The excitation energy dependence of the γ-ray emission is included through the use of generalized Lorentzian forms for the $E1$, $M1$, and $E2$ strength functions. Width fluctuation corrections are applied to the GNASH calculation. The Moldauer model of WFC are employed. After calculation of the population of the first compound nucleus using the Hauser-Feshbach expressions, corrections for preequilibrium and direct reaction effects are made. The preequilibrium contribution calculations were performed using the exciton model in the GNASH code. The one adjustable parameter, the damping matrix element, was taken as 170 MeV^3, based on the comparison of the composite neutron emission spectrum with the spectrum at 14.1 MeV. Multiple preequilibrium emission was included using the model of Ref. [19], and does not include any adjustable parameters. Finally, direct reactions for neutron inelastic scattering were included for scattering to the 2_1^+ state in ^{48}Ti using the distorted-wave Born approximation. The deformation parameters were taken from the compilation given in the International Atomic Energy Agency Reference Input Parameter Library [20], and the neutron optical potential described above.

The spin distribution of the preequilibrium reactions in the residual nucleus is calculated using the quantum mechanical theories of Feshbach, Kerman, and Kooning (FKK) with the multistep direct (MSD) approach. The MSD one-step process for preequilibrium reactions are calculated using the "cmc" code. For this calculation, the multistep compound (MSC) spin distribution is assumed to be the same as the compound residual nucleus spin distribution and absorbed into the Hauser-Feshbach calculations. The transferred spin distribution in preequilibrium reactions is calculated for incident neutron energies 15 MeV, 20 MeV, 25 MeV, 30 MeV, and 35 MeV for a ^{48}Ti target. As an example, some of the calculated spin distributions are shown in Figs. 1−4 for the incident neutron energy of 20 MeV. The histograms are the transferred spin populations calculated using the FKK MSD one-step calculation. In order to incorporate the spin distribution into the GNASH code the histograms need smoothing, therefore histograms of the spin distribution are fitted and the spin cut-off parameters are obtained from the fit. Using these inputs, the γ-ray production cross sections were calculated. Throughout this work, this calculation is referred to as GNASH-FKK.

For the (n, n') channel, the effect on three transitions is investigated. First, in Fig. 5 the 2^+ to 0^+ transition is shown; both GNASH and GNASH-FKK show good agreement with the experimental data and are lower than the data for $E_n \geq 15$ MeV. The difference in the spin distribution for these two calculations is not readily apparent in the case of this low spin transition. The second case is the 4^+ to 2^+ transition in the same channel shown in Fig. 6. In this case, the GNASH predictions are somewhat higher than the experimental result for $E_n = 6-11$ MeV. More importantly, the GNASH-FKK is strongly suppressed compared to the GNASH and experimental data. Similarly, for the 6^+ to 4^+ transition in the (n, n') channel shown in Fig. 7, the GNASH-FKK is suppressed at all neutron energies indicating the effect of preequilibrium reaction.

For the $(n, 2n)$ channel, the transition from the first excited state to the ground state is considered. The GNASH-FKK predictions are in much better agreement with data than the GNASH prediction as in Fig. 8.

In order to demonstrate the effect of the difference in spin distribution in the two calculations, the ratios of the partial γ-ray cross section for 6^+ to 4^+ and the total inelastic scattering are considered in Fig. 9. The ratio predicted using the GNASH without taking into account the preequilibrium reaction, is clearly in disagreement with data, i.e., while data decreases with increasing neutron energy, the GNASH prediction keep increasing. After inclusion of the spin distribution calculated using the preequilibrium effects, the ratio is more similar to the data. The difference in magnitude may be improved by further development of the model. The same ratio between the 4^+ to 2^+ transition cross section and the total inelastic cross section is shown in Fig. 10. The GNASH and GNASH-FKK calculations predict a shape similar to the measured ratio. However, the GNASH prediction tends to increase with increasing neutron energies, while the experimental data tend to be constant with increasing neutron energy. When the spin distribution in the preequilibrium reaction is included, the ratio is much closer to the experimental data. This clearly demonstrates the importance of including the effect of preequilibrium reactions.

V. CONCLUSION

Excitation functions of prompt γ rays produced in the n+^{48}Ti reactions have been measured using the GEANIE spectrometer at the LANSCE/WNR facility. The individual γ-ray yields have been converted to partial transition cross sections as a function of incident neutron energy, by accounting for neutron flux, sample thickness, deadtime corrections, detector and fission chamber efficiencies, and internal conversion processes. The experimental data are presented for neutron energies up to 35 MeV. γ rays from a total of 13 different isotopes were observed and prominant partial γ-ray cross sections were extracted. These partial γ-ray cross sections are com-

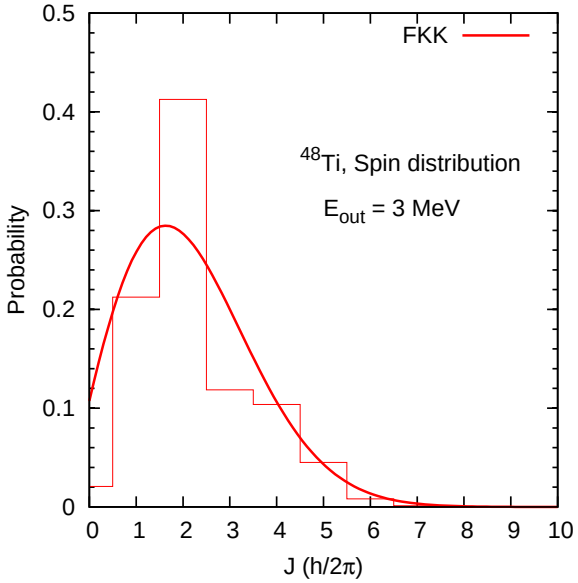

FIG. 1: Spin distribution of the ^{48}Ti + n reaction for incident neutron energy of 20 MeV and outgoing neutron energy of 3 MeV.

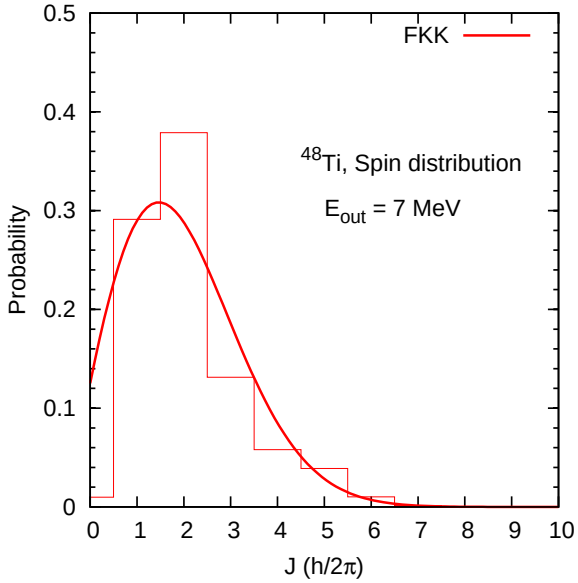

FIG. 2: Spin distribution of the ^{48}Ti + n reaction for incident neutron energy of 20 MeV and outgoing neutron energy of 7 MeV.

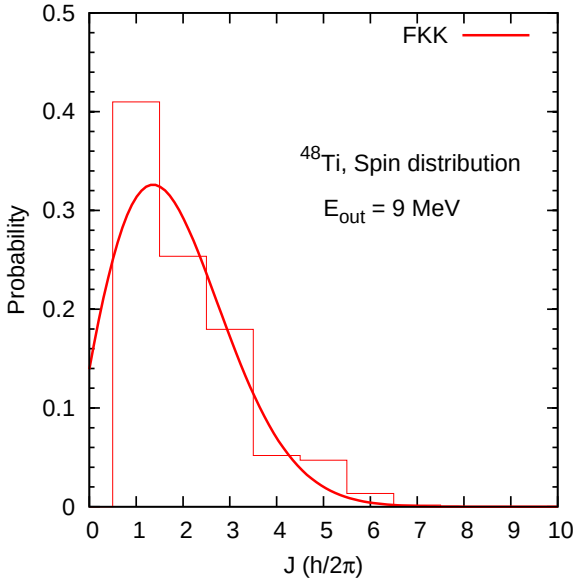

FIG. 3: Spin distribution of the ^{48}Ti + n reaction for incident neutron energy of 20 MeV and outgoing neutron energy of 9 MeV.

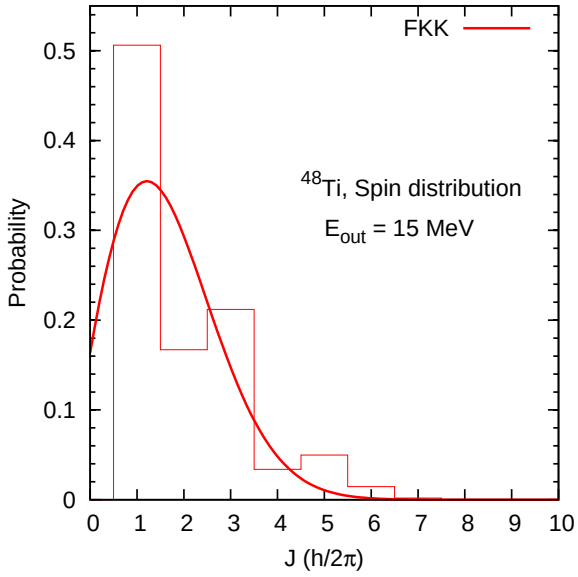

FIG. 4: Spin distribution of the ^{48}Ti + n reaction for incident neutron energy of 20 MeV and outgoing neutron energy of 15 MeV.

pared with the calculations of the GNASH reaction code. The spin distribution of the preequilibrium process in ^{48}Ti + n reactions was calculated for the first time with the quantum mechanical theory of Feshbach, Kerman, and Kooning (FKK). The FKK one-step process was included for the multistep direct (MSD) reaction to account for the preequilibrium effect and the spin cut-off parameters of residual system were estimated. The FKK spin distribution of preequilibrium was incorporated into the GNASH calculations and the γ-ray production cross sections were calculated and compared with experimental data. The difference in the spin distribution with and without preequilibrium effects is significant. The probability of γ transitions from a high spin state is strongly

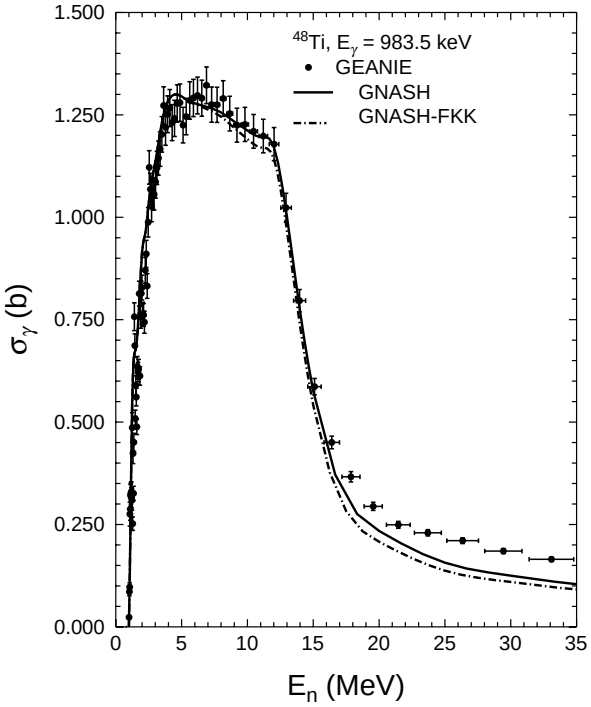

FIG. 5: Partial cross section for E_γ = 983-keV transition between 2^+ to 0^+ in the yrast band of ^{48}Ti. The experimental data are compared with GNASH and GNASH-FKK calculations.

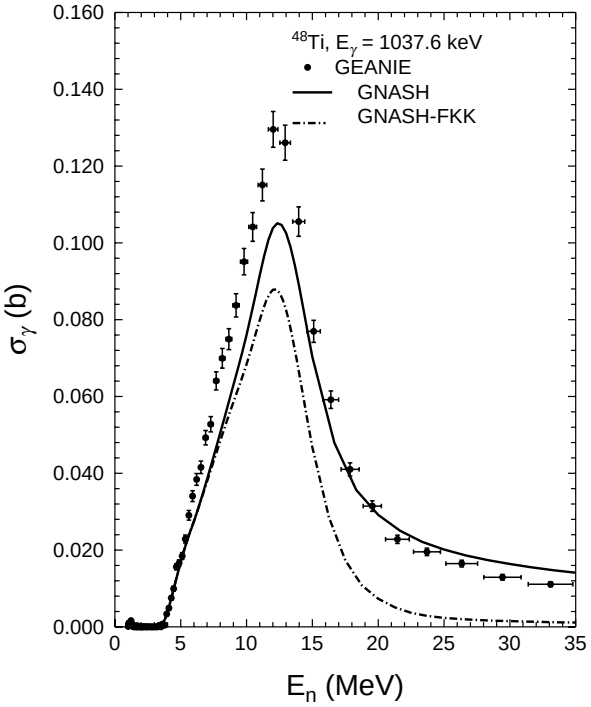

FIG. 7: Partial cross section for E_γ = 1037-keV transition between 6^+ to 4^+ in the yrast band of ^{48}Ti. The experimental data are compared with GNASH and GNASH-FKK calculations.

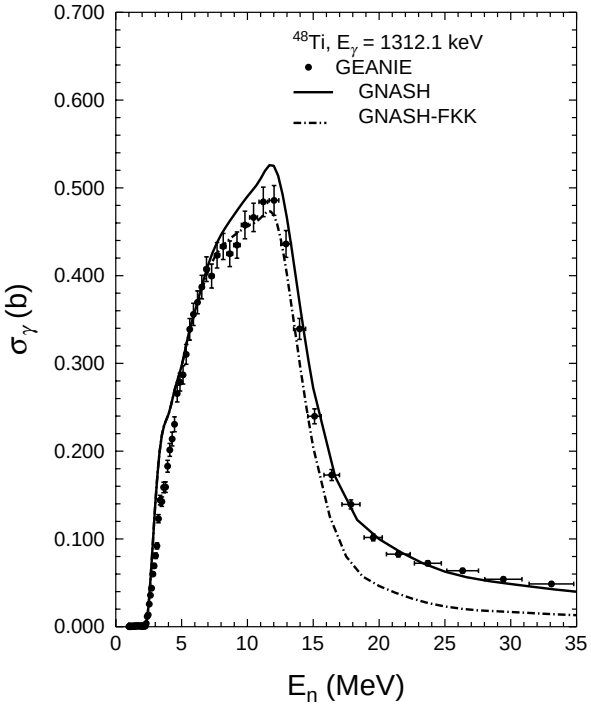

FIG. 6: Partial cross section for E_γ = 1312-keV transition between 4^+ to 2^+ in the yrast band of ^{48}Ti. The experimental data are compared with GNASH and GNASH-FKK calculations.

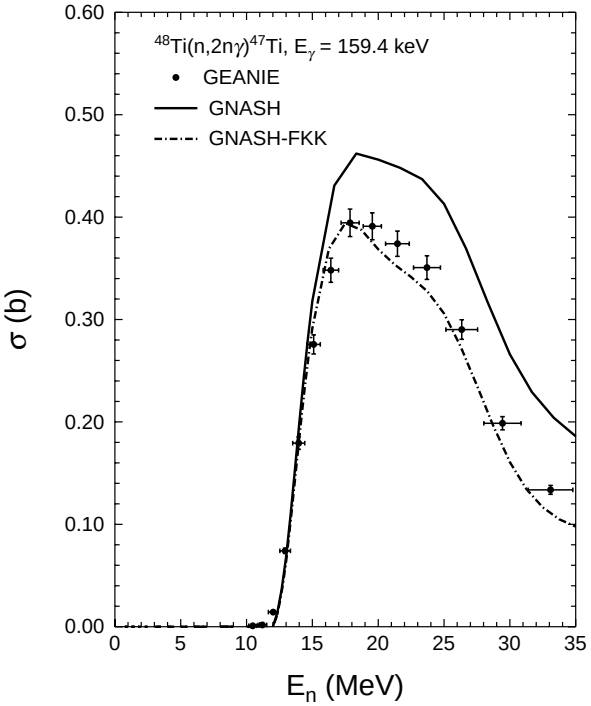

FIG. 8: Partial cross section for E_γ = 159.4-keV transition between $7/2^-$ to $5/2^-$ in the yrast band of ^{47}Ti. The experimental data are compared with GNASH and GNASH-FKK calculations.

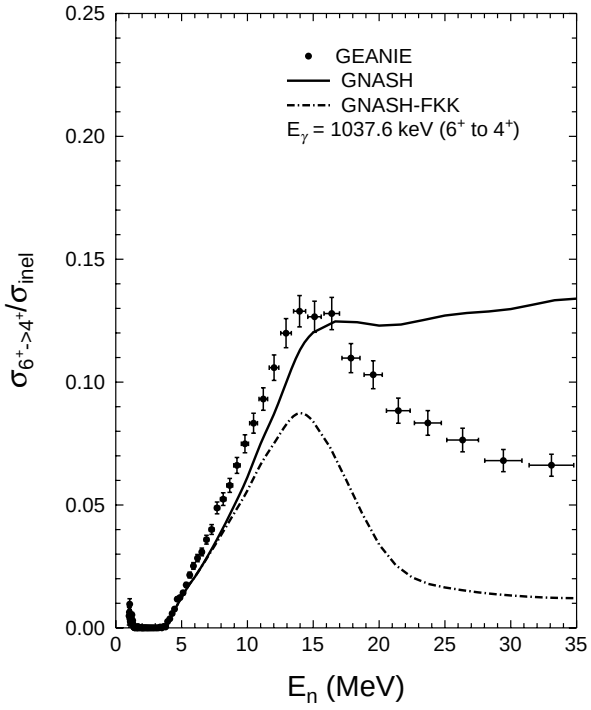

FIG. 9: Ratio of the partial cross section for the 6^+ to 4^+ yrast transition and the total inelastic cross section.

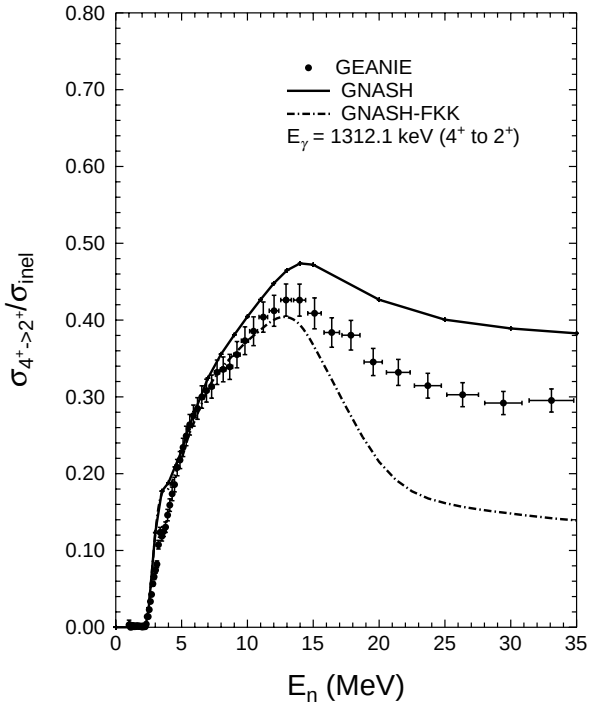

FIG. 10: Ratio of the partial cross section for the 4^+ to 2^+ yrast transition and the total inelastic cross section.

suppressed because of the preequilibrium spin distribution. The statistical properties of preequilibrium reactions are best studied for heavy nuclei far from shell closure where the number of nucleons interacting will be large, thus giving rise to sufficient single particle distributions. This will allow easy coupling of different angular momentum states which in turn will lead to smoother calculated FKK spin distributions. More studies of preequilibrium reactions using heavier nuclei are therefore suggested.

VI. ACKNOWLEDGMENTS

This work was supported in part by the U.S. Department of Energy Grants No. DE-FG03-03NA00076 and No. DE-FG02-97-ER41042, and was performed under the auspices of the U.S. Department of Energy by the University of California, Lawrence Livermore National Laboratory and Los Alamos National Laboratory under contract Nos. W-7405-ENG-48 and W-7405-ENG-36, respectively. This work has benefited from the use of the LANSCE accelerator facility, supported under DOE contract No. W-7405-ENG-36.

[1] H. W. Bertini, Phys. Rev. **131**, 1801 (1963).
[2] J. J. Griffin, Phys. Rev. Lett. **74**, 478 (1966).
[3] H. Feshbach, A. K. Kerman, and S. Koonin, Ann. Phys. (NY) **125**, 429 (1980).

[4] M. Blann, Phys. Rev. **C54**, 1341 (1996).
[5] T. Tamura, T. Udagawa, and H. Lenske, Phys. Rev. **C26**, 379 (1982).
[6] H. Nishioka, H. A. Weidenmüller, and S. Yoshida, Ann. Phys. (N.Y.) **183**, 166 (1988).
[7] D. P. McNabb, Tech. Rep. UCRL-ID-139906, LLNL (1999).
[8] J. F. Briesmeister, Tech. Rep. LA-7396-M-Rev.2, LANL (1986).
[9] S. A. Wender, S. Balestrini, A. Brown, R. C. Haight, C. M. Laymon, T. M. Lee, P. W. Lisowski, W. McCorkle, R. O. Nelson, W. Parker, et al., Nucl. Instrum. Methods Phys. Res. A **336**, 226 (1993).
[10] W. Younes, manuscript in preparation.
[11] National Data Center, Information extracted from the NuDat database, http://www.nndc.bnl.gov/nudat2.
[12] R. O. Nelson, N. Fotiades, M. Devlin, J. A. Becker, P. E. Garrett, and W. Younes, in *International Conference on Nuclear Data for Science and Technology*, edited by R. C. Haight, M. B. Chadwick, T. Kawano, and P. Talou (American Institute of Physics, 2004), p. 838.
[13] D. C. Radford, Nucl. Instrum. Methods Phys. Res. **A361**, 297 (1995).
[14] A. J. Koning and J. P. Delaroche, Nucl. Phys. A **713**, 231 (2003).
[15] F. D. Becchetti and G. W. Greenlees, in *Polarization Phenomena in Nuclear Reactions*, edited by H. H. Barschall and W. Haeberli (University of Wisconsin Press, Madison, 1971), p. 682.
[16] V. Avrigeanu, P. E. Hodgson, and M. Avrigeanu, Phys. Rev. **C 49**, 2136 (1994).
[17] A. V. Ignatyuk, G. N. Smirenkin, and A. S. Toshin, Sov. J. Nucl. Phys. **21**, 255 (1975).
[18] J. Kopecky and M. Uhl, Phys. Rev. **C 41**, 1941 (1989).
[19] M. B. Chadwick, P. G. Young, D. C. George, and Y. Watanabe, Phys. Rev. **C50**, 996 (1994).
[20] T. Belgya, O. Bersillon, R. C. Noy, T. Fukahori, G. Zhigang, S. Goriely, M. Herman, A. V. Ignatyuk, S. Kailas, A. J. Koning, et al., Tech. Rep. IAEA-TECDOC (2004).